Electronic Supplementary Material (ESI) for Journal of Materials Chemistry C.

Supporting Information

Ordered Porous RGO/SnO_2 Thin Films for Ultrasensitive Humidity Detection

Zhou Li,[abc] David W. Gardner,[ab] Yong Xia,[abd] Sikai Zhao,[abe] Aifei Pan,[abd] Nishit Goel,[f] Stephen Bart,[f] Chen Liu,[g] Jianxin Yi,[c] Carlo Carraro,[ab] and Roya Maboudian*[ab]

[a] *Department of Chemical and Biomolecular Engineering, University of California, Berkeley, California, 94720, United States*

[b] *Berkeley Sensor & Actuator Center, University of California, Berkeley, California, 94720, United States*

[c] *State Key Laboratory of Fire Science, Department of Safety Science and Engineering, University of Science and Technology of China, Hefei, Anhui 230026, PR China*

[d] *School of Mechanical Engineering, Xi'an Jiaotong University, Xi'an, Shanxi 710049, PR China*

[e] *School of Resources and Civil Engineering, Northeastern University, Shenyang, Liaoning 110819, PR China*

[f] *TDK InvenSense Inc., San Jose, California, 95110, United States*

[g] *Department of Mechanical Engineering, Stanford University, CA 94305, United States*

* Corresponding author emails: maboudia@berkeley.edu

List of content

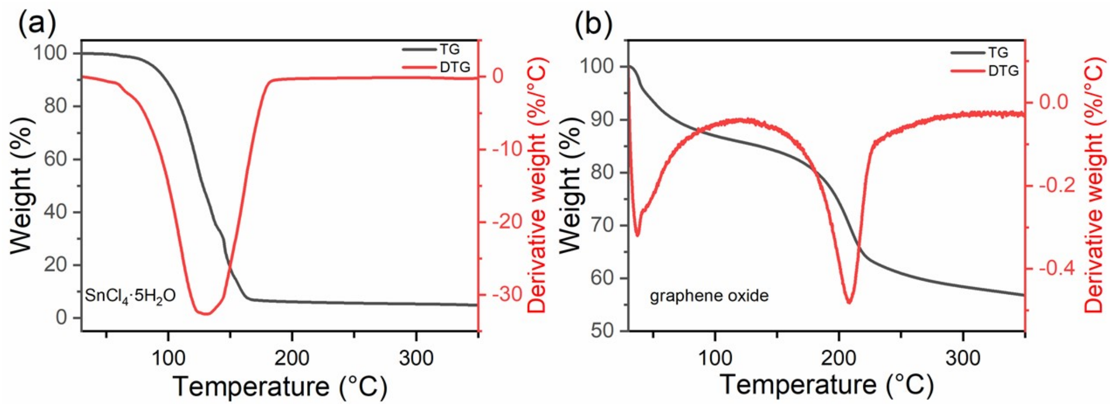

Fig. S1. TGA and DTG analyses of $SnCl_4{\cdot}5H_2O$ and graphene oxide.

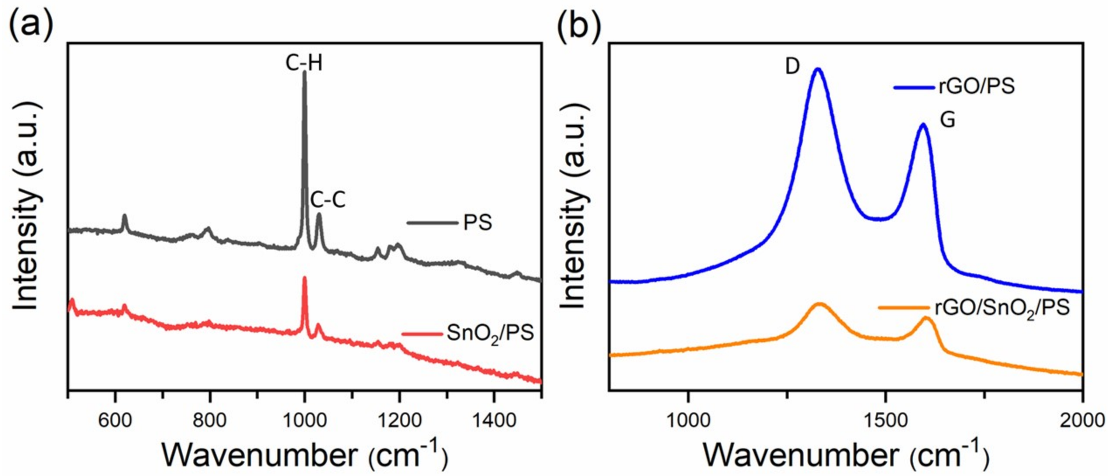

Fig. S2. Raman spectra of PS, SnO_2/PS, rGO/PS, and rGO/SnO_2/PS.

The PS Raman spectrum pattern is measured for comparison shown in Fig. S2a. The two main labeled peaks are consistent with the peaks of related literature [1]. For SnO_2/PS, the main peaks are from PS, indicating the existence of PS. For rGO/PS, and rGO/SnO_2/PS shown by Fig. S2b, no obvious PS peaks are directly observed mainly due to the strong intensity of the rGO peak. However, given the same annealing temperature and time for all these four samples, the existence of PS for rGO/PS, and rGO/SnO_2/PS can be reasonably speculated.

[1] M. Mazilu, A. Luca, A. Riches, C. Herrington, and K. Dholakia, *Opt. Express*, 2010, **18**, 11382-11395.

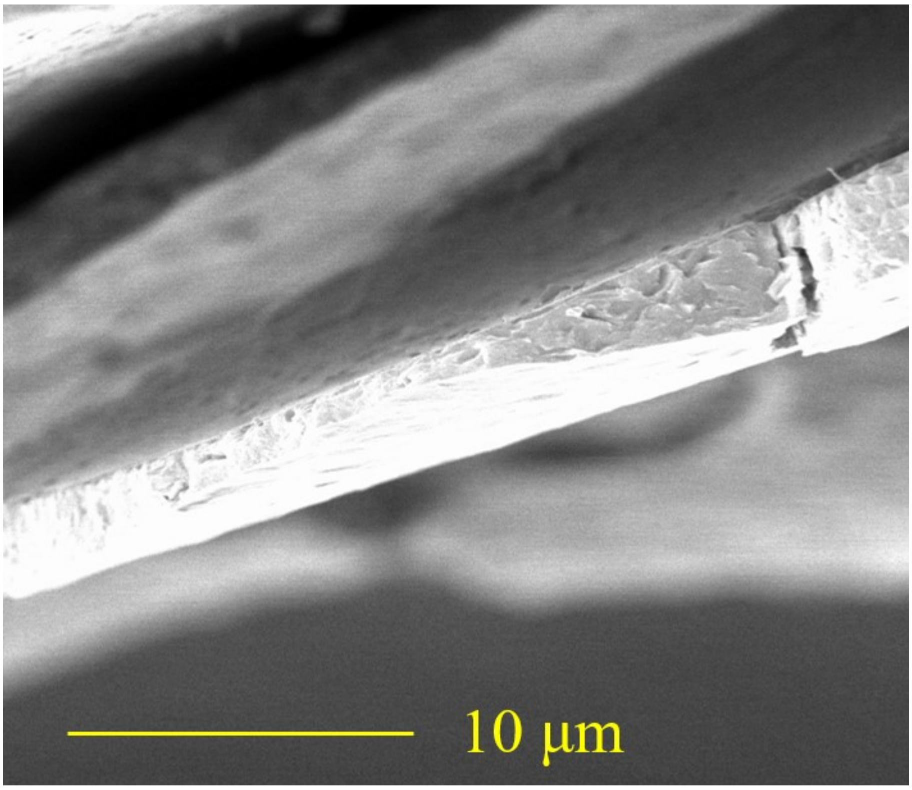

Fig. S3 SEM cross sectional image of rGO/SnO_2/PS.

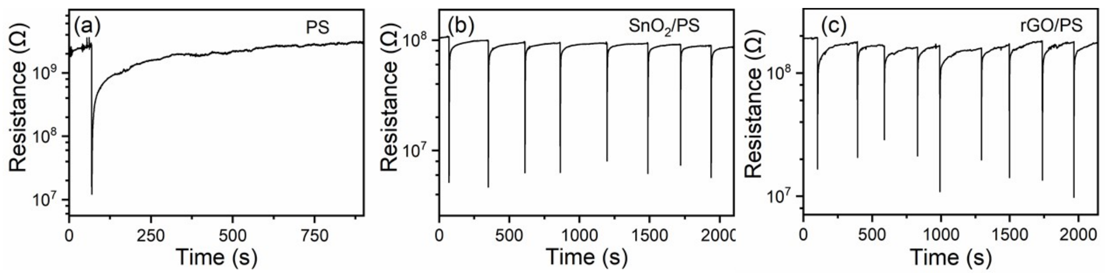

Fig. S4. Dynamic resistance changes of (a) PS, (b) SnO_2/PS, and (c) rGO/PS sensor at an ambient relative humidity of 35% to exhaled breath.

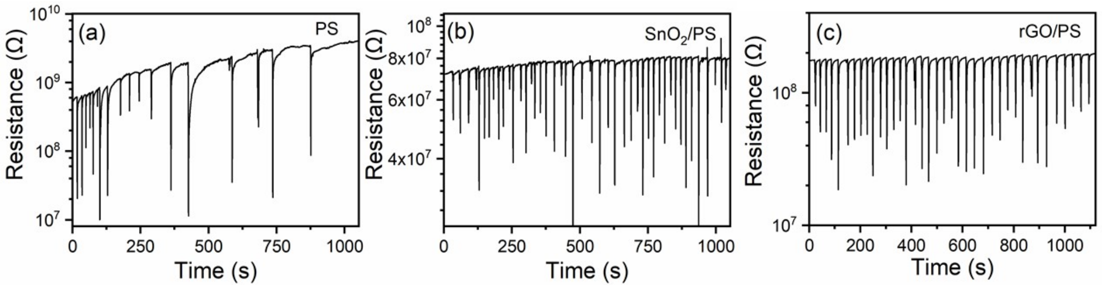

Fig. S5. Dynamic resistance changes of (a) PS, (b) SnO_2/PS, and (c) rGO/PS sensor at an ambient relative humidity of 35% to finger humidity.

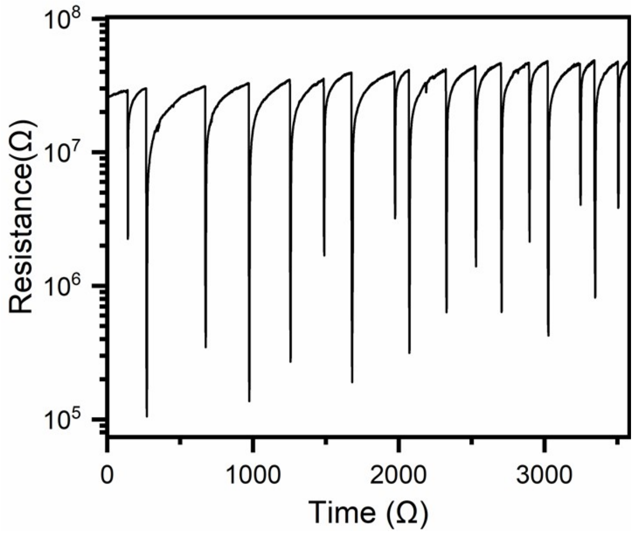

Fig. S6. Repeatability of the sensing performance of rGO/SnO_2/PS sensor to 75% R.H. humidified air at an ambient relative humidity of 25%.

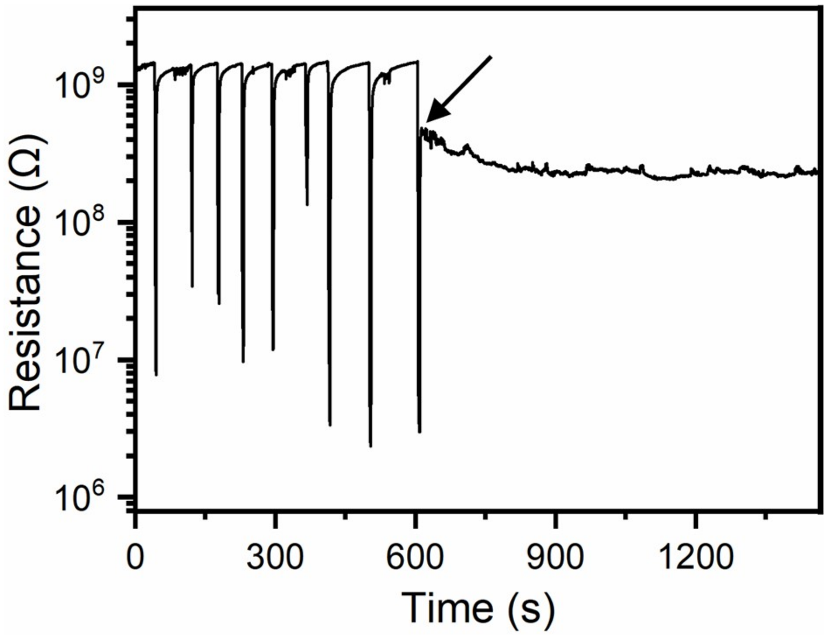

Fig. S7. Repeatability of the sensing performance of rGO/PS sensor to 75% R.H. humidified air at an ambient relative humidity of 25%. The resistance of rGO/PS sensor cannot recover to baseline after several measurement cycles.

.

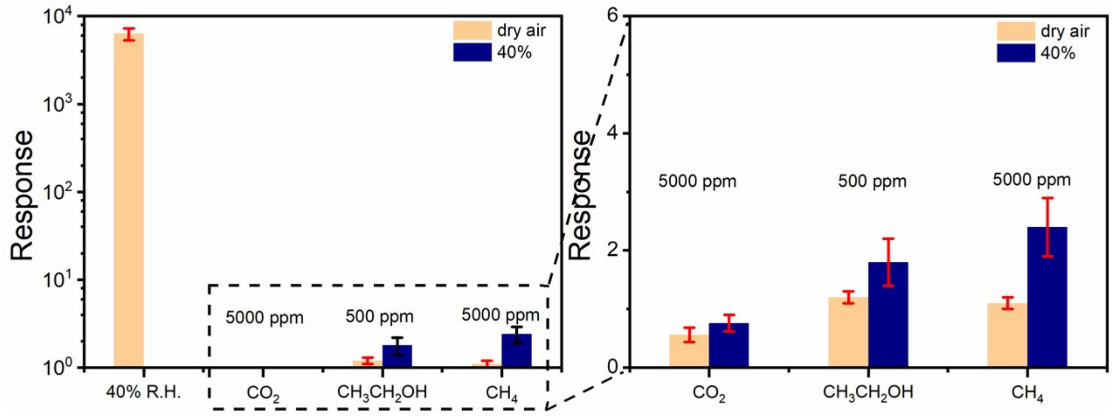

Fig. S8. Responses of rGO/SnO_2 sensor (without PS monolayer template) to 40% R.H. humidified air, CO_2, ethanol, and methane in dry and 40% R.H. humidified air.

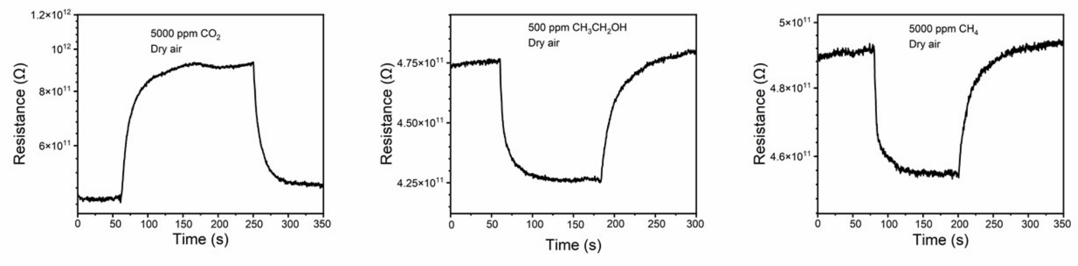

Fig. S9. Response and recovery curves of the rGO/SnO_2/PS sensor to CO_2, CH_3CH_2OH, and CH_4 gases.

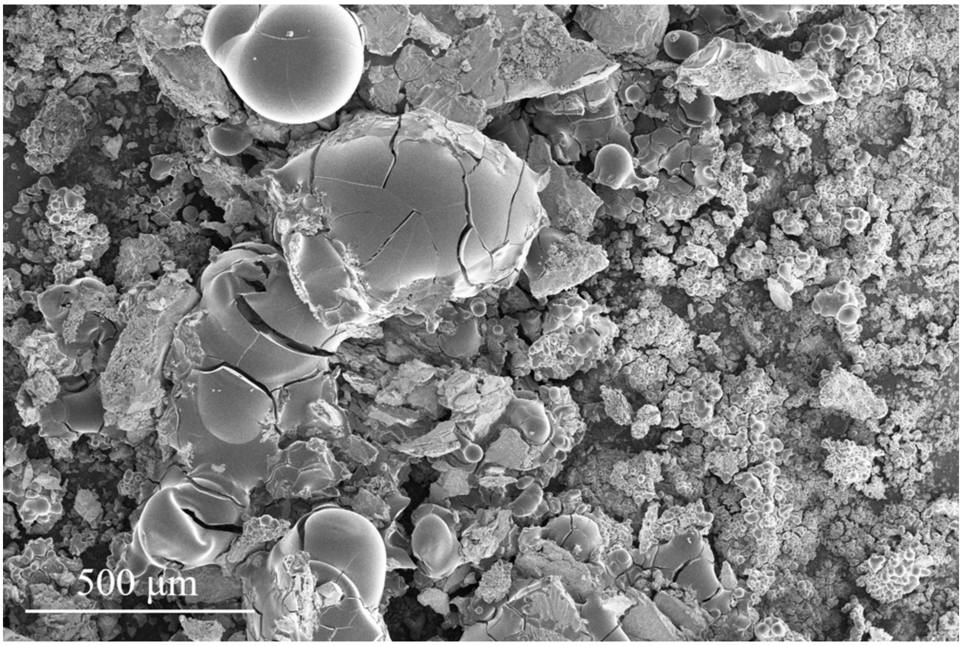

Fig. S10. SEM image of rGO/SnO_2 sensor (without PS monolayer template)

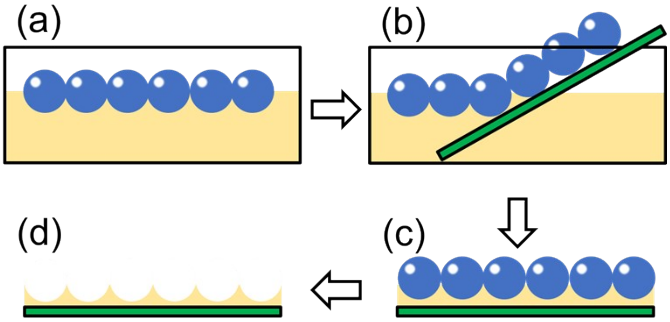

Fig. S11. The synthesis procedure for rGO/SnO_2 porous films. (a) Polystyrene sphere monolayer floats on the precursor solution; (b) The monolayer is picked up by sensor consisting of alumina substrate with Au interdigitated electrodes; (c) The substrate covered with the monolayer is placed horizontally and dries at room temperature; (d) RGO/SnO_2 ordered porous films are formed after annealing at 120°C for 3 h.

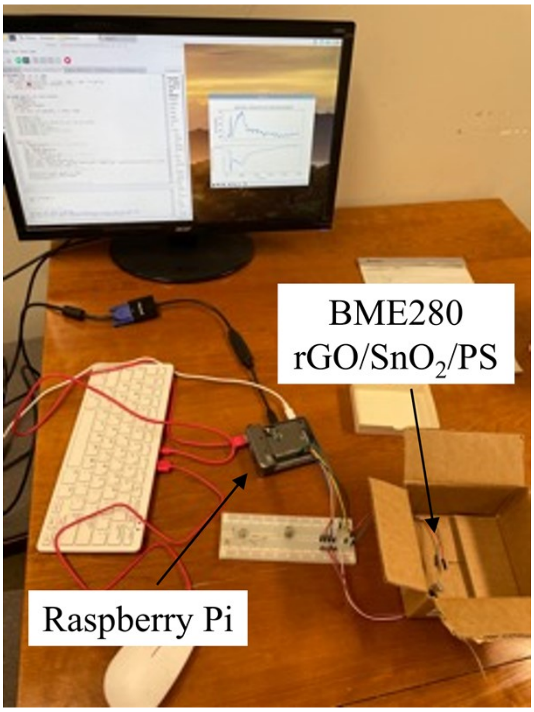

Fig. S12. Long-term test system based on Raspberry Pi.

Table S1 Comparison of Characteristics of Related Humidity Sensors

Material	R. H.	Response	Response time (s)	Ref.
Graphene	95%	0.31	0.6	2
rGO film	100%	0.07	600	3
PDDA/rGO	97%	37.4	108-147	4
rGO/MoS_2	85%	2494	6.3	5
rGO/MoS_2	90%	0.23	17	6
rGO/SnO_2/PS	75%	6300	1.4	This work

[2] N. Agmon, Chem. Phys. Lett., 1995, 244, 456–462.

[3] A. Lipatov, A. Varezhnikov, P. Wilson, V. Sysoev, A. Kolmakov and A. Sinitskii, Nanoscale, 2013, 5, 5426–5434.

[4] A. D. Smith, K. Elgammal, F. Niklaus, A. Delin, A. C. Fischer, S. Vaziri, F. Forsberg, M. R˚asander, H. Hugosson and L. Bergqvist, Nanoscale, 2015, 7, 19099–19109.

[5] S.Y. Park, Y.H. Kim, S.Y. Lee, W. Sohn, J.E. Lee, D.H. Kim, et al., J Mater Chem A, 2018, 6, 5016-5024.

[6] S.Y. Park, J.E. Lee b, Y.H. Kim, J.J. Kim, Y.S. Shim, S.Y. Kim, M.H. Lee, H.W. Jang, Sensor Actuat B-Chem, 2018, 258, 775–782